

Analyzing Land Use/Land Cover Change Using Remote Sensing and GIS in Mosul District, Iraq

Amal Muhammad Saleh¹, Firas W. Ahmed²

^{1,2}College of Agricultural Engineering Sciences, University of Baghdad, Iraq

Email: ¹amalsaleh@aol.com

Abstract

This study aims investigating land use/land cover changes occurred in in Mosul District, Iraq between 2013 and 2020 using remote sensing and GIS. Comparing, two NDVI statistics shows that the most important changes have occurred in low and medium density classes for both periods. The category of low NDVI density has increased from 0.24% in 2013 to about 8.53% in 2020. While the category of medium NDVI density has decreased from 96.40% in 2013 to 88.48% in 2020. Due to the agriculture management and water allocation strategies. Moreover, supervised classification of Landsat 8 OLI images has been employed using maximum likelihood technique. Comparing between the classified images indicate that a considerable increase in rocks cover from 0.25% in 2013 to 2.23% in 2020. The second major category of land in the study area is grassland cover which has increased from 25.80% in 2013 to 39.99% in 2020. Accuracy of the classification has been assessed based on the overall classification accuracy and Kappa coefficient. Thus, the present study illustrates that remote sensing and GIS are important technologies for temporal analysis and quantification of spatial phenomena which is otherwise not possible to attempt through conventional mapping techniques.

Key words: Change detection, normalized difference vegetation index (NDVI), Supervised classification, Accuracy Assessment.

INTRODUCTION

Land use/cover is two separate terminologies which are often used interchangeably (Dimiyati et al., 1996). Land cover refers to the physical characteristics of earth's surface, captured in the distribution of vegetation, water, soil and other physical features of the land, including those created solely by human activities e.g., settlements. While land-use refers to the way in which land has been used by humans and their habitat, usually with accent on the functional role of land for economic activities. Remote sensing and Geographical Information Systems

(GIS) are powerful tools to derive accurate and timely information on the spatial distribution of land use/land cover changes over large areas (Rogana and Chen, 2004). GIS provides a flexible environment for collecting, storing, displaying and analyzing digital data necessary for change detection (Demers, 2008). Remote sensing imagery is the most important data resources of GIS. Satellite imagery is used for recognition of synoptic data of earth's surface (Ulbricht and Heckendorf, 1998).

With the continuous development of remote-sensing technology, the image space and time resolution of remote sensing are continually increasing, and remote-sensing image processing is presenting new challenges. The method for classification commonly used in remote-sensing images is maximum likelihood classifier (Rahman, 2016). The maximum likelihood classification of Landsat 8 satellite data is a method to extract features of a land cover into certain classes. Landsat 8 contains multispectral bands which are visible and infrared bands. The combination of certain bands is able to classify the features of the classes such as water, vegetation and built-up land. Vegetation indices calculated from Landsat 8 satellite data can be used for monitoring temporal changes associated with vegetation. The normalized difference vegetation index (NDVI) is developed for estimating vegetation cover from the reflective bands of satellite data. Moreover the created NDVI images could be used to identify the pattern of changes that had occurred between two different dates (Sahebjalal and Dashtekian, 2013). The aim of the study is to analyze Land use/Land cover change using satellite imagery and GIS in Mosul District, Iraq. Maximum likelihood classification and change detection comparison strategy was employed to identify Land use/Land cover change.

MATERIALS AND METHODS

Study area

Mosul is a major city in northern Iraq. Located approximately 400 km (250 mi) north of Baghdad, and 170 km (110 mi) southeast of the city of Cizre in Turkey, Mosul stands on the west bank of the Tigris (Fig. 1). It is geographically situated on latitude 35° 33' 54.67"-36° 32' 03.79" North and longitude 42° 43' 12.46"-43° 03' 21.78" East. Mosul covers approximately 433537.56 ha of land with the elevation of 271 to 203 m above sea level . The mean annual rainfall of the area is 383.5 mm, while the mean annual temperature is 20.6°C. The surface of Mosul plateau is dissected by shallow valleys with hills rising to 400 meters above the sea surrounding valleys. Fertile soils together with an adequate amount of winter rain provide a good basis for agricultural land use. The Climate is very hot and dry with low rainfall

generally < 75 or 100 mm which is not sufficient to maintain continuous plant cover (Iraqi Meteorological Organization and Seismology).

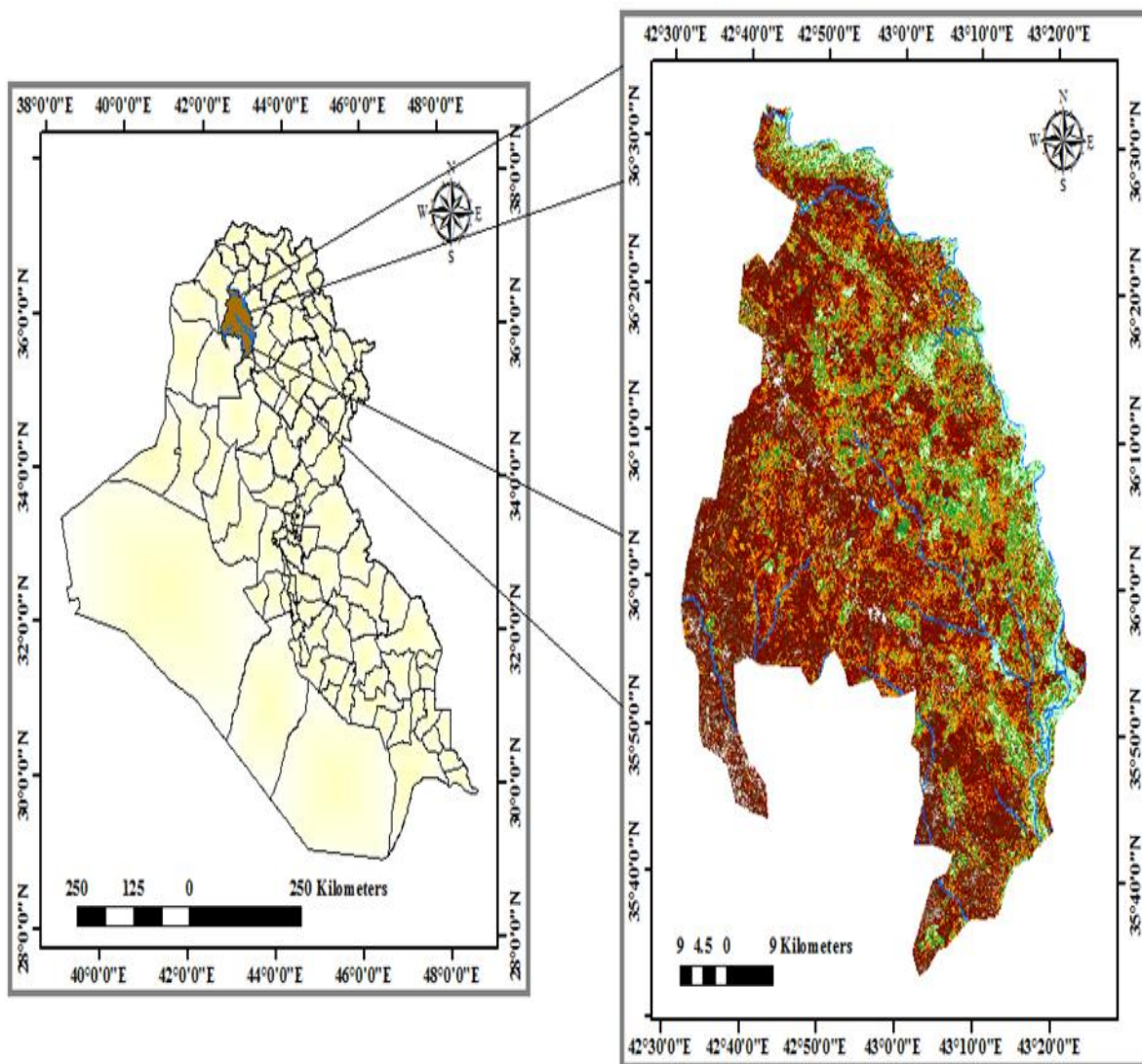


Figure 1. Location of the study area.

Data collecting

Two cloud-free Landsat 8 OLI images acquired on 26th September 2013 and 29th September, 2020 were used for land use/cover classification. The satellite data covering study area were obtained from earth explorer site (<http://earthexplorer.usgs.gov/>). The dates of both images were chosen to be as closely as possible in the same vegetation season. Band combinations were performed in order to obtain visual of interpretation of classes and other information. All visible, near infrared and Panchromatic bands were included in the analysis.

Image processing

Layer stacking at a resolution of 15 m was fulfilled to get images with band combination. Remote sensing image processing was performed using ERDAS Imagine 9.2 and Geographic Information Systems ArcGIS 10.4.1 software. Some corrections have been done to reduce atmospheric effect in the image. Landsat 8 needs to be calibrated by applying a normalization procedure reflectance rescaling factors. The metadata file of Landsat provides information to calculate top of atmosphere reflectance values (TOA). The sub-setting of satellite images were performed for extracting study area from both images by taking geo-referenced outline boundary of Mosul District, the selected area of interest (AOI) were chosen as training pixels.

Image classification

To work out the land use/land cover classification, supervised classification method with maximum likelihood algorithm was done to produce land cover. It is conducted based on verified result. Supervised classification is one of the most methods to detect land use types. Supervised classification is a process where the user selects representative samples for each land cover class in the digital image. These sample land cover classes are called training data. The classification of land cover is based on the spectral signature defined in the training set. The digital image classification software determines each class on what it is similar to most in the training set.

Accuracy of classification

Accuracy assessment was critical for a map generated from any remote sensing data. Error matrix is the most common way to present the accuracy of the classification results (Fan et al., 2007). Overall accuracy, user's and producer's accuracies, and the Kappa statistic were then derived from the error matrices. The Kappa statistic incorporates the off-diagonal elements of the error matrices and represents agreement obtained after removing the proportion of agreement that could be expected to occur by chance (Yuan et al., 2005).

Vegetation index

Vegetation index can be used as an indicator to quantify the greenness of plants within satellite data. There are several vegetation indices, but the most frequently used index is the Normalized Difference Vegetation Index (NDVI) (Rouse et al., 1973). By analyzing images recorded from visible red and near-infrared (NIR) wavelengths. NDVI can be expressed as:

$$NDVI = \frac{NIR - RED}{NIR + RED}$$

In order to the investigation of changes in NDVI values, the NDVI image density was sliced to the nine categories included: areas with low, medium, high NDVI values (Morales et al., 2004).

Change detection

Band math was then performed on the resulting NDVI images by subtracting the 2020 image values from the 2013 image values to find the areas where the land cover has changed. The resultant image was threshold based on 1% changes and the areas with 1% increase or decrease in NDVI values were demonstrated.

Classified image pairs of two different periods data were compared using cross-tabulation in order to determine qualitative and quantitative aspects of the changes for the periods from 2013 to 2020. A change matrix was produced with the help of ERDAS Imagine software. Quantitative area data of the overall land use/Land cover changes as well as gains and losses in each category between 2013 and 2020 were then compiled (Weng, 2001).

Finally, In order to investigate the changes in each land cover type, the overlay consisting of Land use/Land cover change maps of 2013 and 2020 were made through IDRISI Selva 17.02 software. Then a transition matrix was prepared for the overlaid Land use/cover change maps of 2013 and 2020.

RESULTS AND DISCUSSION

NDVI Land cover

The NDVI have been used widely to examine the relation between spectral variability and the changes in vegetation growth rate. It is also useful to determine the production of green vegetation as well as detect vegetation changes. When soil water availability decreases, due to any environmental reason (stress by water deficit); the green vegetation tends to disappear, then the values of NDVI decreases. For this study NDVI calculation was performed to produce NDVI images for both periods. The NDVI values were categorized as low, medium, high densities. Table (1) shows the NDVI density classes in the years 2013 and 2020. In the year 2013, The result indicates that water bodies and river covered an area of 0.15% at the range from -0.98 to -0.43, low NDVI density ranged from -0.43 to -0.02 covered 0.24% while the greatest increase was in medium NDVI density covered 96.40% at the range from -0.02 to 0.17 (Fig. 2). It can be observed that there is a decrease in the high NDVI density at the range from 0.17 to 0.83 covering an area of 3.19%. In the year 2020, water bodies and river covered

an area of 0.29% at the range from -0.56 to -0.15, low NDVI density covered 8.53% at the range from -0.15 to 0.11 (Fig. 3). The most area of medium NDVI density covered 88.48% at the range from 0.11 to 0.20 followed by dense vegetation NDVI values ranged from 0.20 to 0.79 covering an area of 2.70%. The pattern of change evidently resulted from human interferences and its negative effects on natural resources. These pressures are related to worse use of lands, which leads to degeneration of many arable lands in the study area.

As a result the most important changes have occurred in low and medium density classes (Fig. 4). The category of low NDVI density has increased from 0.24% in 2013 to about 8.53% in 2020. In contrast, the category of medium NDVI density has reduced from 96.40% to 88.48%. These results reflect the effect of semiarid climatic conditions and human activities.

Change detection

Change detection is a good indicator for characterizing and understanding changes occurring during any study period (Fig. 5). The change detection which was performed using ERDAS Imagine 9.2 are categorized in the following manner as decreased, some decreased, some increase, and increased (Table 2). Out of the total 251876.16 hectare area, decreased category is in 2nd position, about 21.13% of land surface was changed in between the year 2013-2020, this changes ran across the land surface with randomly distribution followed by some decrease category shows 3rd position which was 17.02%. Some increase category shows top most position about 34.86% of land surface and noticed in the northern and southern areas. A small percentage of land surface showing increasing trend than its previous period which was 9.91%, this changes was noticed in the south-western and north-eastern areas. The remaining 17.07% of land surface is in 4th position found as unchanged category. From the above, it is concluded that the relationships between human activities and natural factors (climate, transportation, weathering, erosion and precipitation) are the determinant factors for dynamics of vegetation changes in the study area.

NDVI density classes	2013 NDVI classes area		2020 NDVI classes area		Change between 2013 and 2020		Average rate of change	
	ha	%	ha	%	ha	%	ha/yr	%
Low NDVI - Low Variability	666.63	0.15	1270.71	0.29	604.08	90.62	86.30	12.95
Low NDVI - Medium Variability	704.61	0.16	431.37	0.10	-273.24	-38.78	-39.03	-5.54
Low NDVI - High Variability	356.22	0.08	36565.20	8.43	36208.98	10164.78	5172.71	1452.11
Medium NDVI - Low Variability	30883.86	7.12	113413.68	26.16	82529.82	267.22	11789.97	38.17
Medium NDVI - Medium Variability	219036.96	50.52	174207.60	40.18	-44829.36	-20.47	-6404.19	-2.92
Medium NDVI - High Variability	168040.62	38.76	95965.74	22.14	-72074.88	-42.90	-10296.41	-6.13
High NDVI - High Variability	8820.72	2.03	7006.41	1.62	-1814.31	-20.57	-259.19	-2.94
High NDVI - Medium Variability	3241.26	0.75	2989.98	0.69	-251.28	-7.75	-35.90	-1.11
High NDVI - Low Variability	1786.68	0.41	1686.87	0.39	-99.81	-5.58	-14.26	-0.80
Total	433537.56	100.00	433537.56	100.00	-----	-----	-----	-----

Table 1. Change of the NDVI density categories between 2013 and 2020.

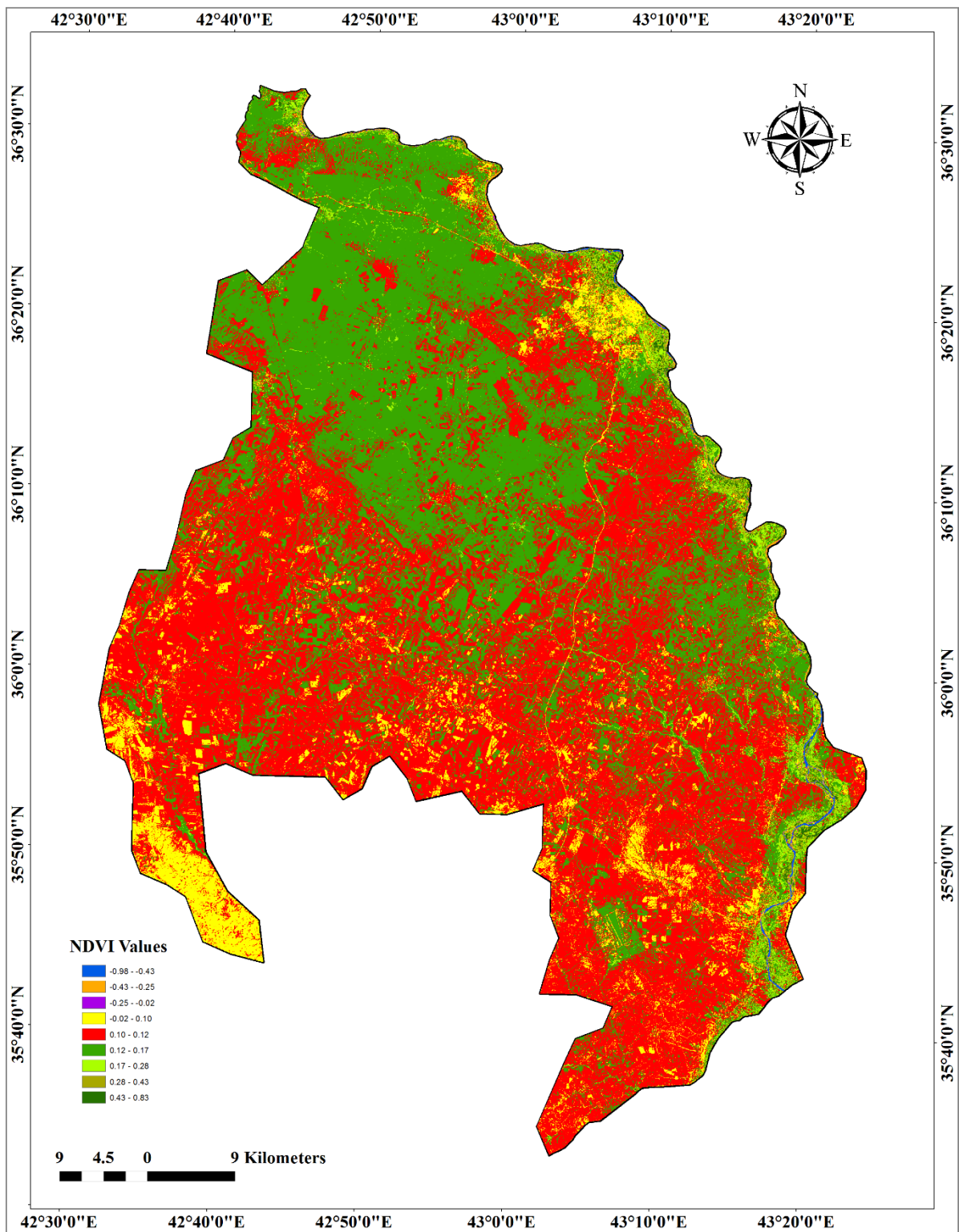


Figure 2. NDVI density categories map of 2013.

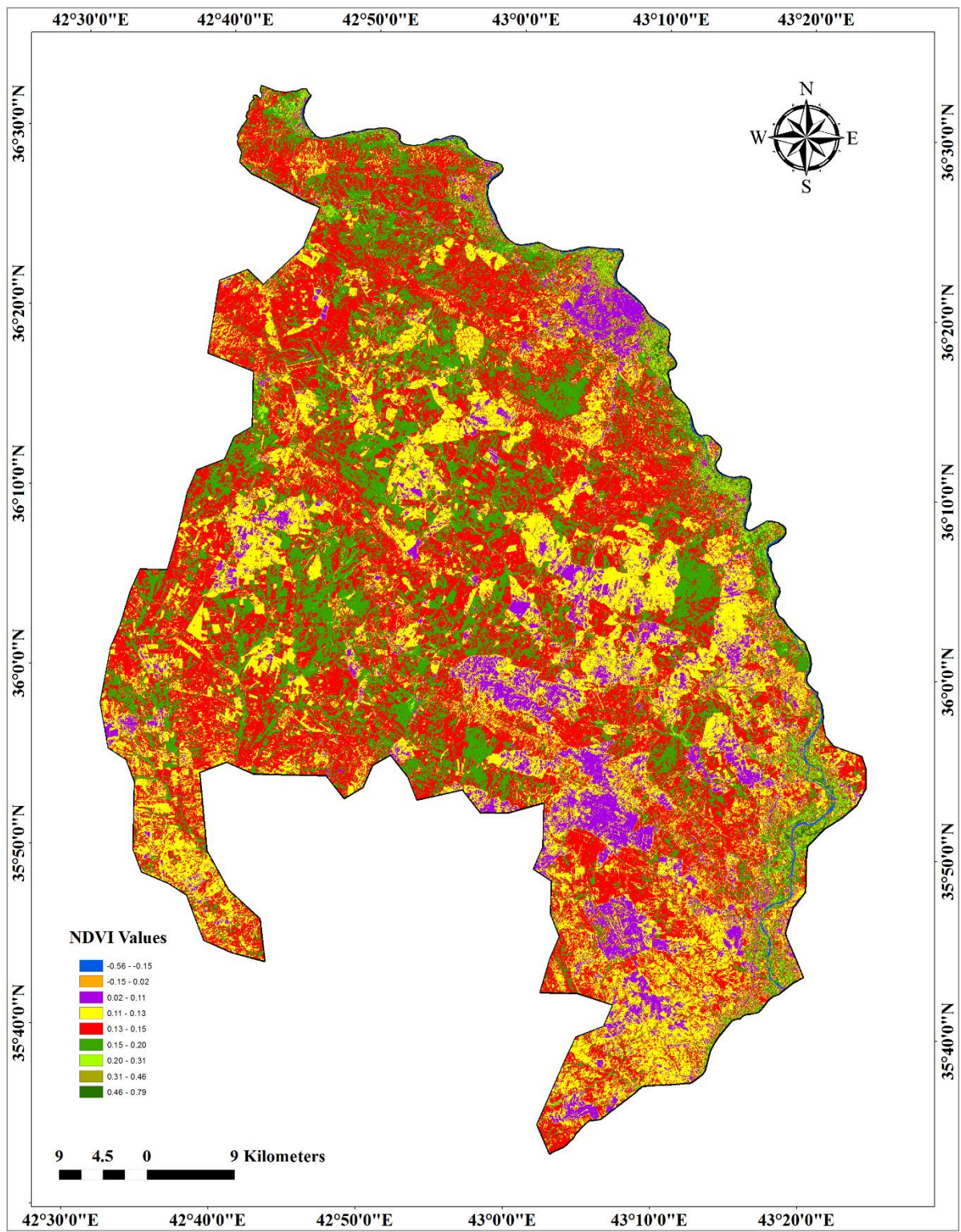


Figure 3. NDVI density categories map of 2020.

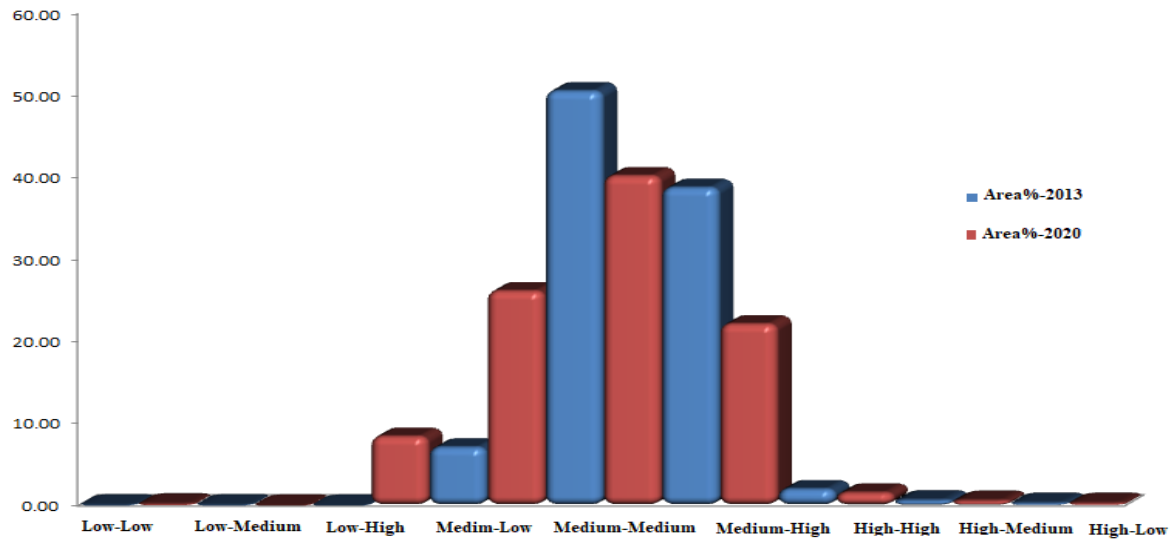


Figure 4. Changes of NDVI density categories during the period of 2013 to 2020.

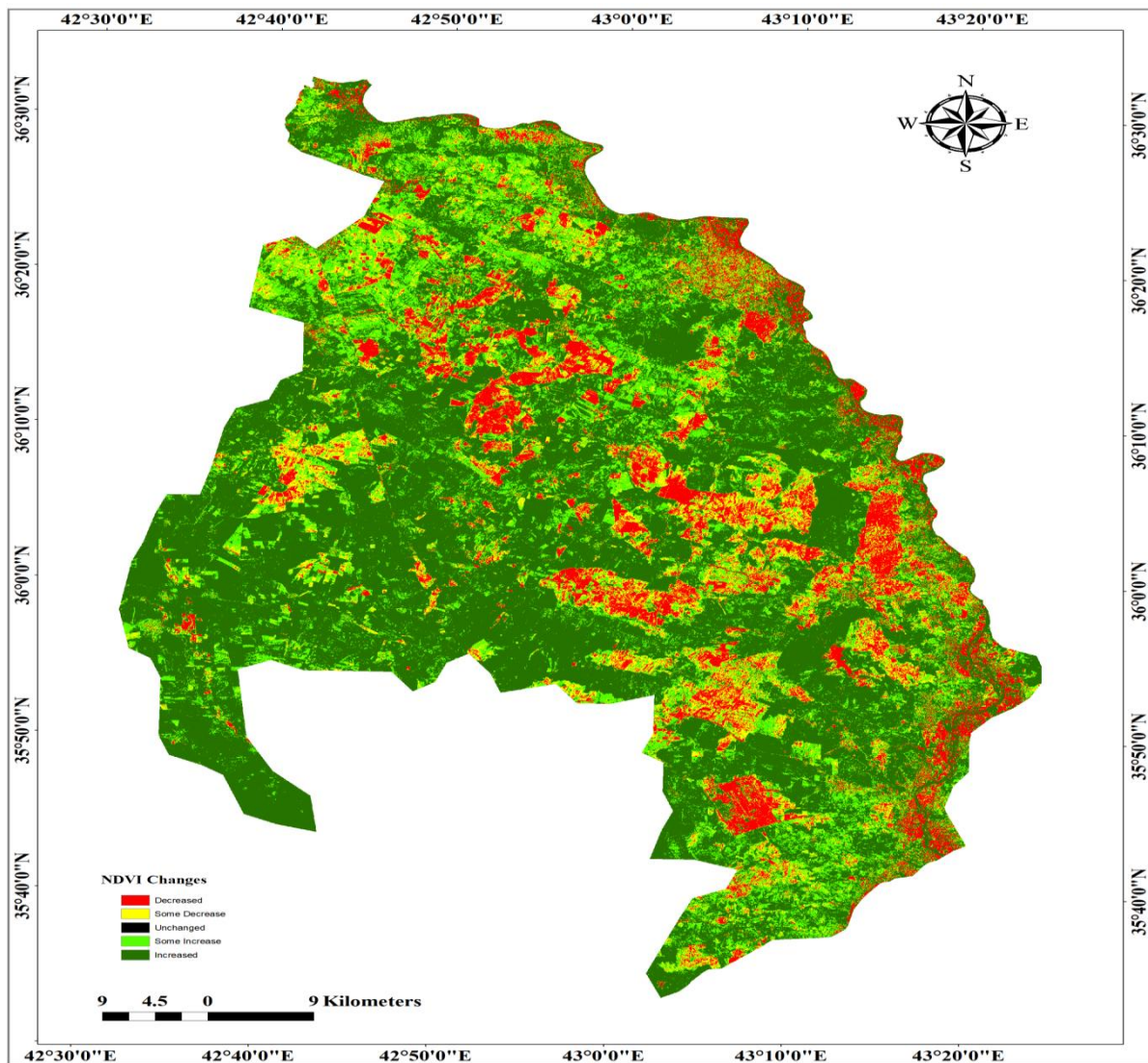


Figure 5. Threshold NDVI difference map.

Table 2. NDVI changes during the seven-years period.

NDVI changes	Area_ha	Area%
Decreased	53221.59	21.13
Some Decrease	42878.52	17.02
Unchanged	43005.51	17.07
Some Increase	87807.60	34.86
Increased	24962.94	9.91
Total	251876.16	100

Image classification

In this study, totally, seven Land use/Land cover classes were established as rocks, urban, bare soils, hills, grassland, agriculture and water (Table 3). In the supervised classification technique, two images with different dates are independently classified. In the year 2013, bare soils are the most dominant land-cover class in the study area. It covers less than half of the total land surface (shares of 45.70%) at the center of the study area toward north-western part and few areas of southern regions of the study area (Fig. 6). Due to retraction the water level in Tigris river. Grassland cover is at the 2nd position (shares of 25.80%) found in the southern and south-eastern areas. Whereas hills cover is at the 3rd position (shares of 16.09%) ran across the land surface toward Tigris river. In the year 2020, grassland cover shows top most position (shares of 39.99%) at the center of the study area toward north-western part and few areas of southern and south- eastern regions of the study area (Fig. 7). Bare soils are at the 2nd position (shares of 39.01%) found in the northern, north-eastern and south eastern areas. While hills cover is at the 3rd position (shares of 10.14%) found along Tigris river and few areas of northern regions of the study area.

Land use/Land cover change

Data registered in Table (3) and Fig. (8) reveal that both positive and negative changes occurred in the land use/land cover pattern of Mosul District, During the seven years, The exposed rock category includes areas of bedrock exposure, scarps, talus, slides, and other accumulations of rocks represented by sedimentary rocks that are exposed in the study area, which belong to different geological formations. It has increased from 0.25% in 2013 to 2.23% in 2020 which accounts for 802.00% of the total study area. Grassland has increased from 25.80% in 2013 to 39.99% in 2020 which accounts for 55.00%. Water has decreased from 7.40% in 2013 to 3.85% in 2020 which accounts for -48.04%. Due to the construction of dams on the river to impound water, leads to changes in the flow regime of the river upstream the reservoir due to backwater flow. Impounding causes increase of the flow cross sectional area leading to a decrease in the flow velocity and the ability of the river to transport sediment. Hills has decreased from 16.09% in 2013 to 10.14% in 2020 which accounts for -36.97%. These results reflect the effect of climatic conditions, and soil erosion by wind and water (geomorphic processes). Vegetation has increased from 1.72% in 2013 to 2.12% in 2020 which accounts for 23.17%. Due to wheat and barley cultivation.

Table 3. Comparison of areas and rates of changes in LULC classes between 2013 and 2020.

LULC type	2013 LULC area		2020 LULC area		Change between 2013 and 2020		Average rate of change	
	ha	%	ha	%	ha	%	ha/yr	%
Rocks	1074.83	0.25	9695.00	2.23	8620.17	802.00	1231.45	114.57
Urban	13202.15	3.04	11539.55	2.66	-1662.60	-12.59	-237.51	-1.80
Bare Soils	198248.90	45.70	169241.54	39.01	-29007.36	-14.63	-4143.91	-2.09
Hills	69815.86	16.09	44004.49	10.14	-25811.37	-36.97	-3687.34	-5.28
Grassland	111926.54	25.80	173484.74	39.99	61558.20	55.00	8794.03	7.86
Vegetation	7449.73	1.72	9176.09	2.12	1726.36	23.17	246.62	3.31
Water	32106.26	7.40	16682.85	3.85	-15423.41	-48.04	-2203.34	-6.86
Total	433824.26	100	433824.26	100	-----	-----	-----	-----

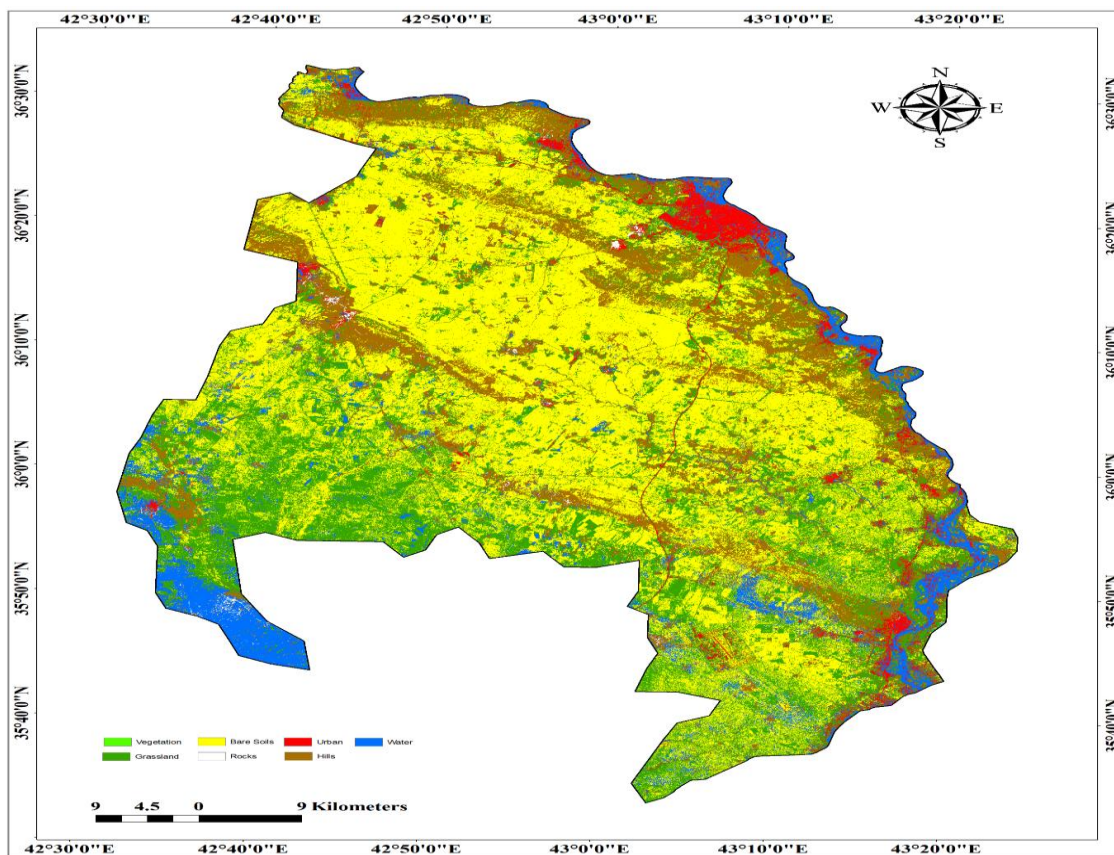


Figure 6. Classified image 2013.

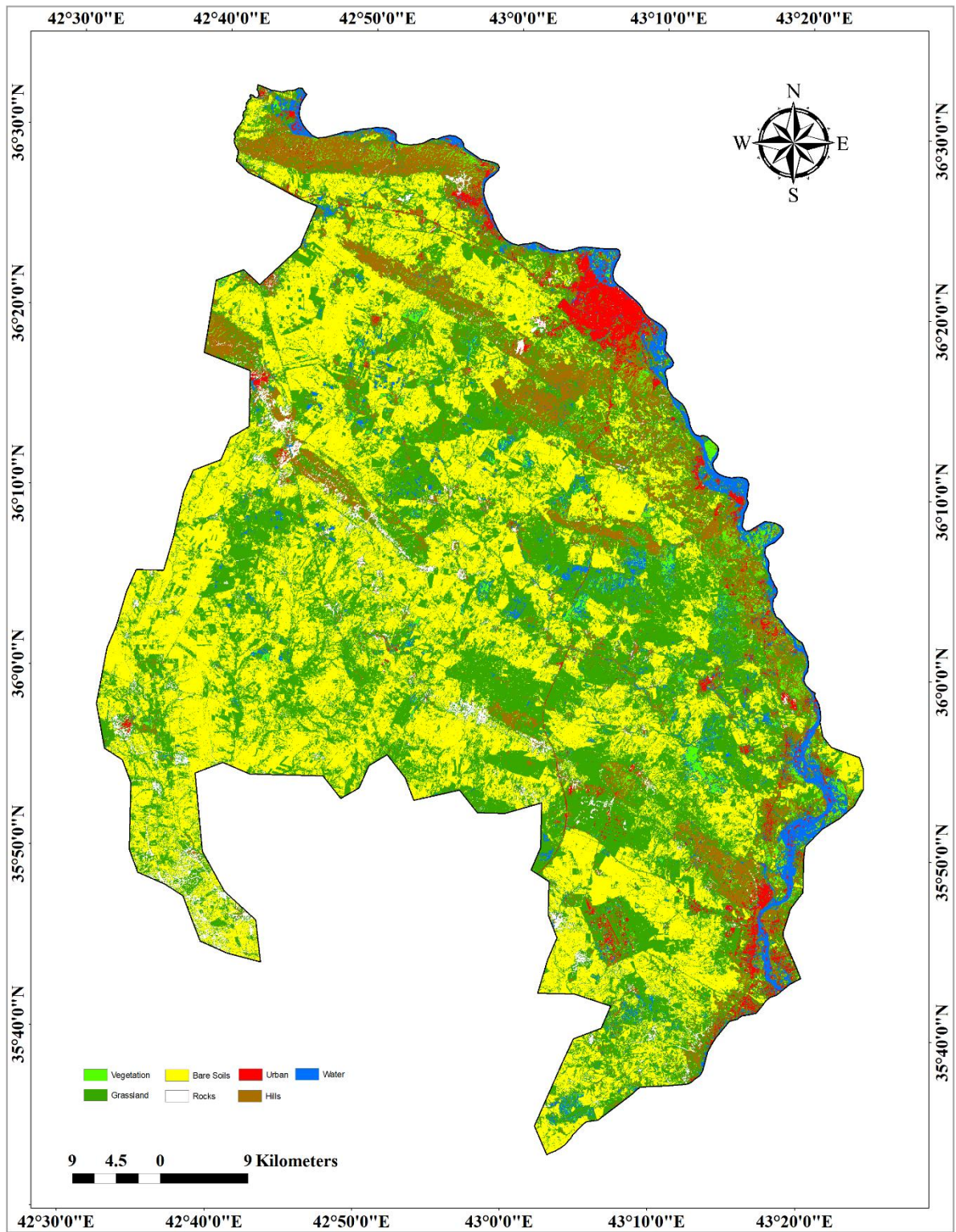


Figure 7. Classified image of 2020.

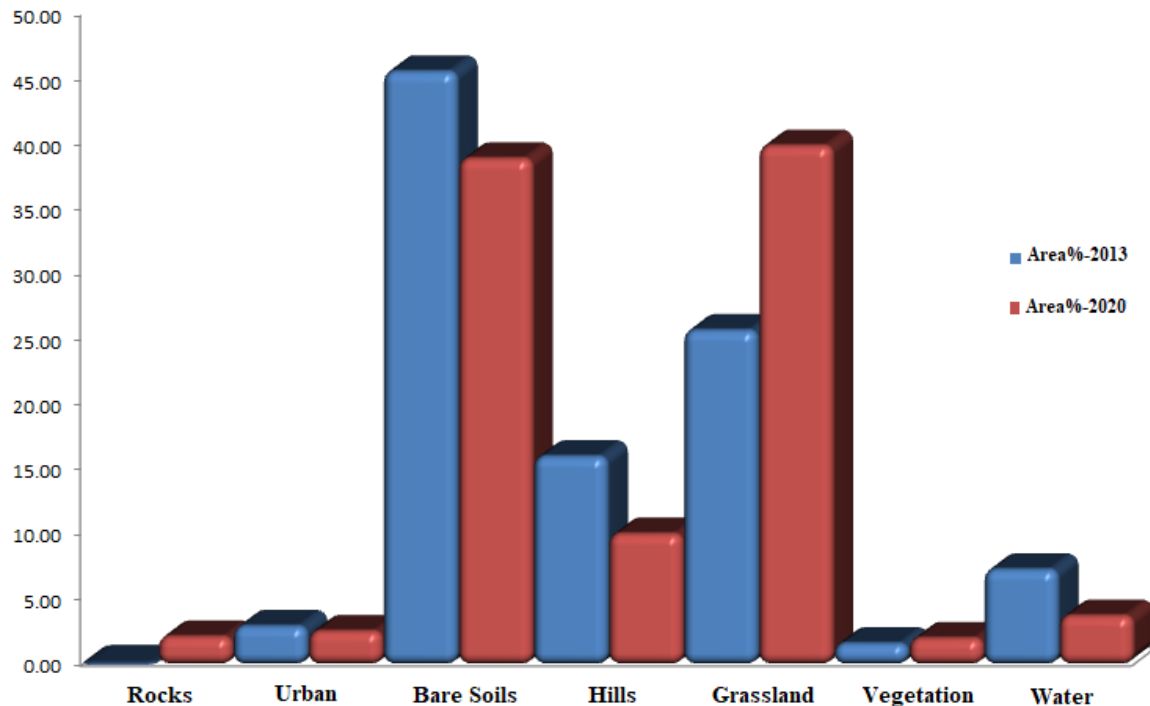


Figure 8. Changes of the land cover categories during the period 2013 to 2020.

Accuracy Assessment

To evaluate the accuracy of the classified images, error matrix was used based on random sampling method (Sahebjalal and Dashtekian, 2013) in which 94 to 97 points were automatically selected from classified reference image in the years 2013 and 2020 respectively.

According to the results, the users' accuracy for the land classes in the year 2013 was the following: vegetation (100%), grassland (94.44%), bare soils (90.48%), urban (100%), hills (66.67%), followed by water (90.00%) (Table 4). While the users' accuracy for the land classes in the year 2020 was the following: vegetation (100%), grassland (73.68%), bare soils (92.86%), rocks (33.33%), hills (81.82%), followed by water (100%) (Table 5). The overall accuracy of classification results were 86.17% ($K = 0.8030$) and 82.47% ($K = 0.7233$) for the year 2013 and 2020, respectively.

The following land classes presented difficulties: bare soils, rocks, and hills. Also vegetation and grassland along Tigris river. Due to their close spectral behaviour, they brought some confusion in classification. On the other hand, water and urban there were no problems given the different spectral behaviour for these land classes (Voroventii and Muntean, 2012). Then, a transition matrix was prepared for the overlaid Land use/Land cover change maps of 2013 and 2020. Fig. (9) shows the thematic map of Land use/Land cover change during the study period.

Table 4. The results from the accuracy assessment process for the image classification of the year 2013. *Overall classification accuracy = 86.17%, *overall Kappa statistics = 0.8030.

Class name	Reference total	Classified totals	Number correct	Producers accuracy (%)	Users accuracy (%)	Kappa index
Vegetation	1	1	1	100.00	100.00	1.0000
Grassland	22	18	17	77.27	94.44	0.9275
Bare soils	43	42	38	88.37	90.48	0.8245
Rocks	0	0	0	-----	-----	0.0000
Urban	2	2	2	100.00	100.00	1.0000
Hills	15	21	14	93.33	66.67	0.6034
Water	11	10	9	81.82	90.00	0.8867
Totals	94	94	81	-----	-----	-----

Table 5. The results from the accuracy assessment process for the image classification of the year 2020. *Overall classification accuracy = 82.47%, *overall Kappa statistics = 0.7233

Class name	Reference total	Classified totals	Number correct	Producers accuracy (%)	Users accuracy (%)	Kappa index
Vegetation	1	1	1	100.00	100.00	1.0000
Grassland	31	38	28	90.32	73.68	0.6132
Bare soils	51	42	39	76.47	92.86	0.8494
Rocks	1	3	1	100.00	33.33	0.3264
Urban	0	0	0	-----	-----	0.0000
Hills	11	11	9	81.82	81.82	0.7949
Water	2	2	2	100.00	100.00	1.0000
Totals	97	97	80	-----	-----	-----

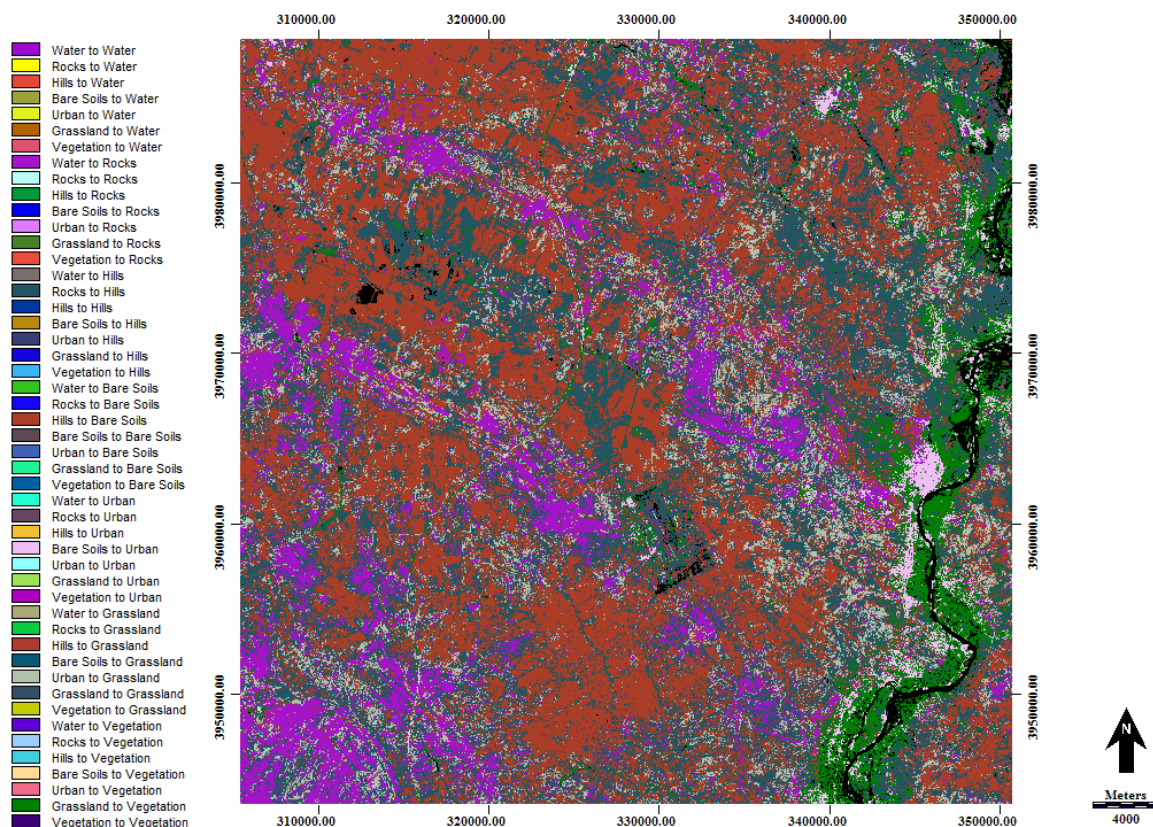


Figure 9. Land use/Land cover change map (2013-2020).

CONCLUSION

1. The change detection analysis is an efficient way of describing the changes observed in each land use category. The normalized difference vegetation index technique is relatively easy to implement and simple to interpret, but it cannot provide complete matrices of change directions (Lu et al., 2004). and the index is also subject to registration error (Gong et al., 1992).
2. The distributions of NDVI for the period 2013-2020 showed positive pattern of low vegetation density (from 0.24% in 2013 to about 8.53% in 2020). While the distributions of medium NDVI density for both period showed negative pattern of (from 96.40% in 2013 to 88.48% in 2020).
3. Supervised classification of Landsat 8 OLI images for both periods is a proper tool to derive land cover/land use maps. A considerable change of Land use/Land cover in rocks was positive during the period 2013-2020 (from 0.25% in 2013 to 2.23% in 2020). Furthermore grassland cover was positive for both periods (from 25.80% in 2013 to 39.99% in 2020.).
4. Several factors have significant impact on Land use/Land cover changes observed during the study period. This is may be due, mainly, to the effect of dry climatic conditions, vegetation, previous farming practices, agriculture management, topographical conditions, geomorphic processe and human activities.

5. . Accuracy of the classification has been assessed based on the overall classification accuracy and Kappa coefficient. The overall accuracy of classification results were 86.17% ($K = 0.8030$) and 82.47% ($K = 0.7233$) for the year 2013 and 2020, respectively.
6. For maintaining ecological balance of this area require further study to examine their vegetation potential and dynamics.

REFERENCE

- a. S. Muhaimed, A. J. Saloom and K. A. Saliem 2014. Classification and Distribution of Iraqi Soils. *International Journal of Agriculture Innovations and Research*. 2(6): 997-1002.
- [2]. Dimiyati, M., Mizuno, K., Kobayashi, S., Kitamura, T., 1996. An analysis of land use/cover change using the combination of MSS Landsat and land use map: a case study in Yogyakarta, Indonesia. *International Journal of Remote Sensing*, 17(5): 931-944.
- [3]. Rogana J., Chen, D. 2004. Remote sensing technology for mapping and monitoring land-cover and land-use change. *Progress in Planning*, 61: 301-325.
- [4]. Demers, M. N. *Fundamentals of Geographic Information Systems*. 2008. Fourth Edition, John Wiley&Sons, Inc., Newyork, USA.
- [5]. Ulbricht, K.A., Heckendorff, W.D. 1998. Satellite images for recognition of landscape and land use changes. *ISPRS Journal of Photogrammetry and Remote Sensing*, 53(4): 235-243.
- [6]. M. T. Rahman. 2016. Detection of land use/land cover changes and urban sprawl in Al-Khobar, Saudi Arabia: an analysis of multi-temporal remote sensing data. *ISPRS International Journal of Geo-Information*, 5(2): 15; <https://doi.org/10.3390/ijgi5020015>
- [7]. E. Sahebjalal and K. Dashtekian. 2013. Analysis of land use-land covers changes using normalized difference vegetation index (NDVI) differencing and classification methods. *African Journal of Agricultural Research*. 8(37):4614-4622
- [8]. Fan, F., Weng, Q., Wang, Y. 2007. Land use land cover change in Guangzhou, China, from 1998 to2003, based on Landsat TM/ETM+ imagery. *Sensors*, 7: 1323-1342.
- [9]. Yuan, F., Sawaya, K.E., Loeffelholz, B.C., Bauer, M.E. 2005. Land cover classification and change analysis of the Twin Cities (Minnesota) metropolitan areas by multitemporal Landsat remote sensing. *Remote Sensing of Environment*, 98: 317-328.
- [10]. J. W. Rouse, R. H. Haas, J. A. Schell, and D. W. Deering. (1973). Monitoring the vernal advancement and retrogradation (green wave effect) of natural vegetation.
- [11]. Morales L, Castellaro G, Sobrino J A and Kharraz J E 2004. Land Cover Dynamic Monitoring in the Region of Coquimbo (Chile) by the Analysis of Multitemporal NOAA-AVHRR NDVI Images. Web site:
- [12]. https://www.researchgate.net/publication/228888999in_the_region_of_Coquimbo_Chile_by_the_analysis_of_multitemporal_NOAA-AVHRR_NDVI_images/figures?lo=1
- [13]. Weng, Q. 2001. A remote sensing-GIS evaluation of urban expansion and its impact on surface temperature in the Zhujiang Delta, southern China. *International Journal of Remote Sensing*, 22(10): 1999-2014.

- [14]. Ehsan Sahebjalal and Kazem Dashtekian. 2013. Analysis of land use-land covers changes using normalized difference vegetation index (NDVI) differencing and classification methods, African Journal of Agricultural Research. 8(37):4614-4622.
- [15]. Iosif Vorovencii and Mihaela Denisa Muntean. 2012. Evaluation Of Supervised Classification Algorithms For Landsat 5 Tm Images.
- [16]. <https://www.researchgate.net/publication/313584971>
- [17]. Lu D, Mausel P., Brondizio E., Moran E. 2004. Change detection techniques. International Journal of Remote Sensing. 25:2365-2407.
- [18]. Gong P, Ledrew EF, Miller JR 1992. Registration-noise reduction in difference images for change detection. International Journal of Remote Sensing. 13:773–779.